Lawrence Berkeley National Laboratory

Title

Field Quality of the 4.5-m-Long MQXFA Pre-Series Magnets for the HL-LHC Upgrade as Observed During Magnet Assembly

Permalink

https://escholarship.org/uc/item/4tn523mk

Authors

Wang, X
Ambrosio, G
Yahia, A Ben
et al.

Peer reviewed

Field Quality of the 4.5 m-Long MQXFA Pre-Series Magnets for the HL-LHC Upgrade As Observed During Magnet Assembly

X. Wang, G. Ambrosio, A. Ben Yahia, D. W. Cheng, J. DiMarco, P. Ferracin, W. Ghiorso,
S. Izquierdo Bermudez, C. Myers, H. Pan, S. O. Prestemon, K. L. Ray, G.L. Sabbi, M. Solis

Abstract—The U.S. High-Luminosity LHC Accelerator Upgrade Project (HL-LHC AUP) is developing MQXFA magnets, a series of 4.5 m long 150 mm aperture high-field Nb_3Sn quadrupole magnets for the HL-LHC upgrade at CERN. Five pre-series magnets, MQXFA03 through MQXFA07, have been developed. During the magnet assembly stage, we perform magnetic measurements on the coil-pack sub-assembly and magnets after loading to track the field quality for two purposes. First, it serves as a quality assurance tool to check if the magnet field quality is on track to meet the acceptance criteria. Magnetic measurements are used to understand if magnetic shims are needed to compensate low-order field errors and to meet the field quality targets. Second, the measurements during the assembly stage can also help understand the field quality, especially the geometric field errors, for Nb_3Sn accelerator magnets. Here we summarize the measurement results of the pre-series MQXFA magnets, including the magnetic axis and twist angle. The results will provide useful feedback for the series production of Nb_3Sn magnets and on the optimization of field quality of accelerator magnets based on the wind-and-react Nb_3Sn technology.

Index Terms—Nb_3Sn, quadrupole magnet, High-Luminosity LHC.

I. INTRODUCTION

IN collaboration with CERN, the U.S. High-Luminosity Large Hadron Collider (LHC) Accelerator Upgrade Project (AUP) is developing Nb_3Sn quadrupole magnets, MQXFA, that will be used at the interaction region of the LHC [1], [2]. The MQXFA magnet is 4.5 m long with an aperture of 150 mm [3]. The magnet consists of four coils made of Nb_3Sn Rutherford cables [4]. After winding, the coils are heat-treated at a peak temperature of 665 °C to form the superconducting Nb_3Sn. The reacted coils are then impregnated with epoxy resin. Details on the coil fabrication are reported in [5].

To assemble the magnet, we first make a coil-pack sub-assembly where the four coils are surrounded by aluminum collars that in turn are surrounded by iron pads [6]. We then

insert the coil pack into the shell-yoke structure and apply the pre-stress to the coils with a bladder-key technique at room temperature, a process called loading [3].

We take at least two magnetic measurements during the assembly stage of the MQXFA magnets to track the field quality: one on the coil-pack sub-assembly and one on the magnet after the loading is completed [6]. The magnetic measurements intend to serve two purposes. First, to check if the magnet field quality is on track to meet the acceptance criteria on the magnetic center and magnetic field angle. The magnetic axis of the MQXFA magnets is a straight line defined by two fiducials, one at each end of the magnet [7]. The local magnetic center is to be within ± 0.5 mm from the magnetic axis in both the horizontal and vertical directions. The local magnetic field angle is to be within ± 2 mrad from the average magnetic field angle of the whole magnet [8]. Based on the measured field errors, we also decide if magnetic shims are needed to compensate low-order field errors and to meet the field quality targets [9]. The second purpose is to help understand the field quality, especially geometric field errors, for Nb_3Sn accelerator magnets more generally.

Here we report the measurement results for the five pre-series magnets MQXFA03–07 [6], [10]. We report the measured main field, magnetic axis and magnetic field angle, followed by the field errors and the impact of loading on the field quality. The results will help understand the field quality of MQXFA magnets, one of the first productions of Nb_3Sn accelerator magnets.

II. MEASUREMENT SYSTEM AND DATA REDUCTION

The measurement coordinate system is described in [7]. The magnetic center is determined by the magnetic measurements and the rotation axis of the probe as determined by the survey. The main-field twist angle is determined by the magnetic measurements and the angle of the encoder index measured by the tilt meter that is mounted next to the encoder.

The magnetic field in the aperture of the MQXFA magnet is expressed as

$$B_y + iB_x = B_2 \times 10^{-4} \sum_{n=1}^{\infty} (b_n + ia_n) \left(\frac{x + iy}{R_{\text{ref}}} \right)^{n-1}, \quad (1)$$

where b_n is the normal and a_n is the skew multipole coefficient of order n, normalized to the main field, B_2, at the magnet center. They are expressed in units at the reference radius

This article has been accepted for publication in IEEE Transactions on Applied Superconductivity. This is the author's version which has not been fully edited and content may change prior to final publication. Citation information: DOI 10.1109/TASC.2022.3156540

2

$R_{\text{ref}} = 50$ mm for the MQXFA magnets [11]. The data reduction followed the procedures as described in [12].

The rotating probe, called Mark #1, has two nominally identical printed-circuit boards (PCBs) developed by FNAL [13]. The effective length of each PCB rotating coil is 108.74 mm. The two PCBs are placed back to back to measure the twist angle of the main field when the back PCB overlaps the front PCB as the probe travels along the magnet. This new measurement method, developed by J. DiMarco of FNAL, is described in [14] with the measurement results.

Three measurement components were changed from the original setup [7]. First, a new power supply was used (CAEN FAST-PS-1K5 30-50). Second, the magnet current was measured with a current transducer (Danisense DS50UB-10) and a digital multimeter (Keithley 2701). Third, the change of the angular position of the encoder-index along the magnet was measured by a digital tilt meter (RST Instruments IC6554).

The measurement protocol was described in [7]. The main change for the pre-series magnets was that the measurement current decreased from ± 15 to ± 10 A. The probe rotated at 3 Hz for magnets MQXFA03–06. The speed decreased to 2 Hz for MQXFA07 to reduce the voltage noise in the slip ring.

III. MEASUREMENT RESULTS

A. Measurement Resolution of the Multipoles

Probe Mark #1 has a resolution of around 0.001 units at the reference radius of 50 mm, as shown in Fig. 1. Allowed multipoles of the order up to $n = 26$ can be distinguished. The resolution is consistent with those of earlier probes with the same or similar rotating coil designs [7], [15].
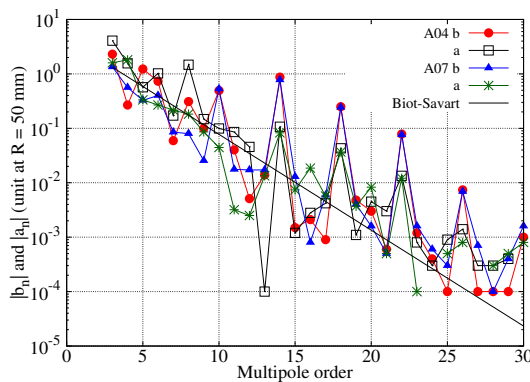

Fig. 1. The absolute values of the normalized multipole coefficients averaged along the straight part of the pre-series magnets MQXFA04 and A07. Also shown is the decay slope of the coefficients given by the Biot-Savart law [16].

B. Main Field Transfer Function

Table I lists the absolute values of the transfer function (TF) and the magnetic lengths for the pre-series magnets. The transfer functions included the integrated TF that is integrated over the magnet length and the central TF that is averaged in the straight part of the magnet.

TABLE I
THE ABSOLUTE VALUE OF THE MAIN FIELD TRANSFER FUNCTION (TF) AND MAGNETIC LENGTH L_{M} FOR THE PRE-SERIES MQXFA MAGNETS. THE NUMBER OF THE SECOND-GENERATION (2G) COILS WITH THE b_6 TUNING IN EACH MAGNET IS ALSO LISTED.

Magnet	2G-b_6 coils	|Integrated TF| (T kA^{-1})	|Central TF| (T m^{-1}kA^{-1})	L_{m} (m)
A03	0	37.198	8.831	4.213
A04	1	37.178	8.828	4.211
A05	4	37.350	8.870	4.211
A06	4	37.290	8.857	4.210
A07	4	37.334	8.868	4.210

C. Magnetic Center in the Straight Part of the Magnet

Table II gives the maximum deviation of the local magnetic centers, in the straight part of the magnet, from the magnetic axis in the horizontal x and vertical y directions. The average deviation in both directions is set to zero. The deviation in both directions are within ± 0.25 mm.

TABLE II
THE MINIMUM AND MAXIMUM DEVIATION OF THE LOCAL MAGNETIC CENTERS FROM THE MAGNETIC AXIS FOR THE PRE-SERIES MQXFA MAGNETS. THE AVERAGE DEVIATION IS SET TO ZERO.

Magnet	x min (mm)	x max (mm)	y min (mm)	y max (mm)
A03	-0.073	0.087	-0.161	0.142
A04	-0.138	0.076	-0.167	0.084
A05	-0.230	0.183	-0.215	0.178
A06	-0.154	0.189	-0.195	0.093
A07	-0.099	0.073	-0.123	0.125

D. Twist Angle of the Main Field

Fig. 2 compares the main-field twist angle of the pre-series magnets. The local twist angles are within ± 2 mrad except for the magnet ends: the lead end region where $z > 1.55$ m and return end region where $z < -1.91$ m.
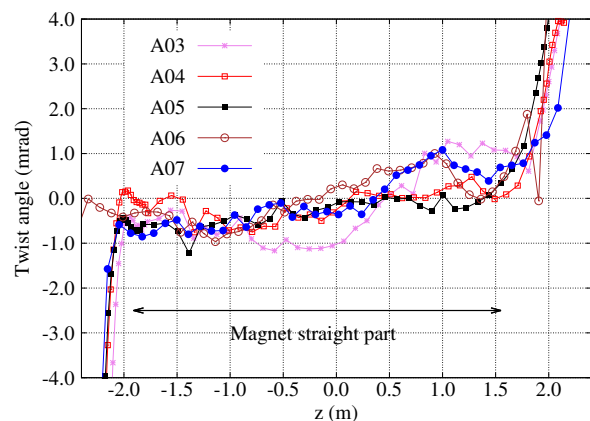

Fig. 2. The main-field twist angle of the pre-series magnets. The average twist angle of each magnet is set to zero.

This article has been accepted for publication in IEEE Transactions on Applied Superconductivity. This is the author's version which has not been fully edited and content may change prior to final publication. Citation information: DOI 10.1109/TASC.2022.3156540

3

E. Geometric Field Errors

Fig. 3 shows the mean values of the field errors in the straight part of the pre-series magnets measured with ± 10 A at room temperature. The sextupoles of three magnets, MQXFA04–06, are about 1.5–2 units out of the bounds; the multipoles of MQXFA07 are fully within the bounds.
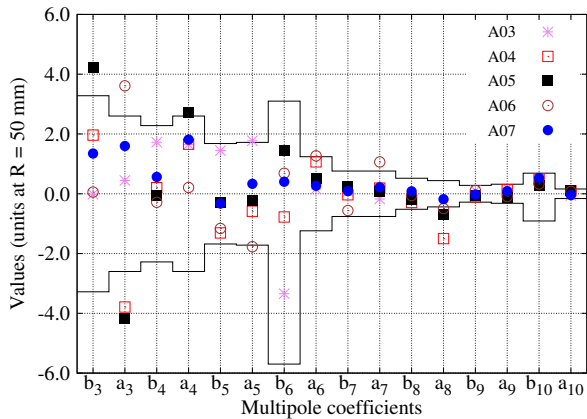

Fig. 3. The field errors in the straight part of the pre-series MQXFA magnets measured with ± 10 A at room temperature. The black lines denote the upper and lower bounds for each multipole coefficient for low current at room temperature [8].

Fig. 4 compares the standard deviation, σ, of the normal and skew field errors in the straight part of each pre-series magnet with the scaling law based on different amplitudes of the root-mean-square (rms) displacement of coil blocks. Assuming a small and rigid displacement of coil blocks, Todesco *et al.* showed that the standard deviation of the field errors in a quadrupole magnet follows a scaling law $\sigma(d) = d\alpha\beta^n$, where d is the rms amplitude of the coil-block displacement, α and β are the fitting parameters, and n is the harmonic order [16]. With the scaling law, one may estimate the positioning error of the coil block based on the measured field errors. For the MQXFA magnets, the Monte Carlo calculation with ROXIE [17] gives that $\alpha = 148.482$ mm^{-1} and $\beta = 0.6192$. The measured σ is consistent with a 60–70 μm rms displacement of the coil blocks.

F. Impact of Loading on Field Quality

Table III lists the changes of the transfer functions of the pre-series magnets and field errors in the straight part of the magnets, after loading and with respect to the coil-pack sub-assembly. The changes in the higher-order multipoles with $n > 6$ are negligible.

Fig. 5 shows the profiles of the transfer function, a_3 and b_6 of MQXFA04 measured on the coil-pack sub-assembly and after loading. The after-loading profiles largely shifted along the y-axis from those of the coil-pack sub-assembly.

Fig. 6 shows the main-field twist angle of MQXFA05 coil-pack sub-assembly and after loading. For z from -2 to 1.5 m, the maximum peak-to-peak value of the twist angle decreased from about 3 mrad in the coil-pack sub-assembly to about 1 mrad after loading. The impact on the magnetic center is unknown as the coordinates of the probe rotation axis are not surveyed for the coil-pack sub-assembly.
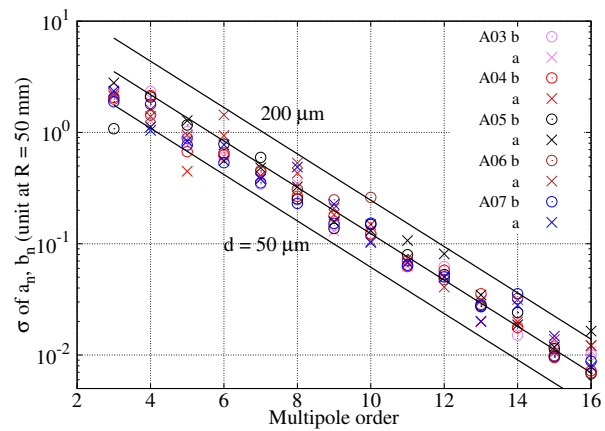

Fig. 4. The standard deviation of multipoles in the straight section of the pre-series magnets indicates an rms displacement of $60 - 70$ μm. The solid lines represent three rms displacements: top: $d = 200$ μm; middle: $d = 100$ μm; bottom: $d = 50$ μm.

TABLE III
THE CHANGES OF THE TRANSFER FUNCTIONS AND LOW-ORDER FIELD
ERRORS AFTER LOADING, WITH RESPECT TO THE VALUES OF THE
COIL-PACK SUB-ASSEMBLY, FOR THE PRE-SERIES MAGNETS. THE TF AND
MULTIPOLES ARE EXPRESSED IN UNITS.

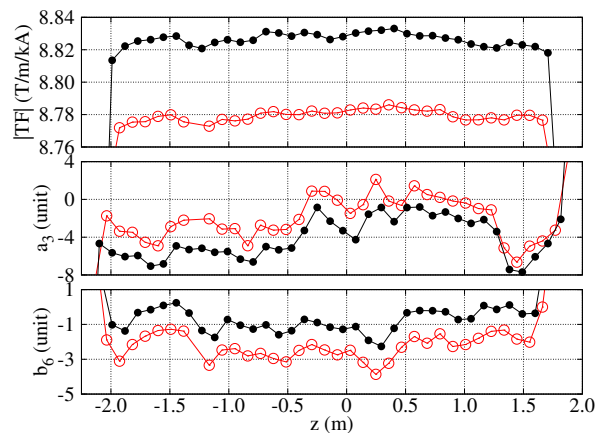|	A03	A04	A05	A06	A07
Integrated TF	68	70	60	75	70
Central TF	51	60	44	61	53
a_3	-1.50	-2.13	-0.75	-0.45	-0.98
a_4	-0.24	-0.59	0.75	-0.99	-0.33
a_5	-0.21	-0.13	0.20	-0.02	0.29
b_3	-1.61	-0.47	0.61	0.33	1.71
b_4	-0.20	0.60	-0.09	0.49	0.03
b_5	-0.02	0.00	0.10	0.01	-0.19
b_6	1.30	1.53	1.75	1.64	1.44

Fig. 5. The measured main-field transfer function in absolute value, a_3 and b_6 of the MQXFA04 magnet. Red open circles: coil-pack sub-assembly; black solid circles: after loading.

IV. MEASUREMENTS VERSUS REQUIREMENTS

Table I shows that the measured central transfer function is within 0.4% of 8.858 T m^{-1} kA^{-1}, the expected value with the nominal MQXFA cross section based on the second-generation coils. The difference is less than 0.2% for MQXFA05–07. The magnetic length measured at room temperature is about 0.3%
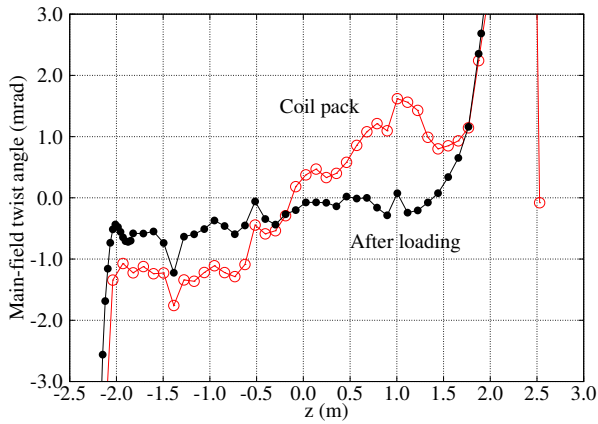
Fig. 6. The measured main-field twist angle of MQXFA05. Red open circles: coil-pack sub-assembly. Black solid circles: after loading.

higher than 4.2 m, the expected magnetic length at 1.9 K [9].

The maximum deviation of the magnetic centers from the magnetic axis are well within ± 0.5 mm for the pre-series magnets (Table II), meeting the acceptance criterion [8]. Unlike the magnetic centers, the local twist angle is out of the ± 2 mrad bounds toward the connection side of the magnets (Fig. 2). The twist angle is measured over about 109 mm probe length. If one averages the twist angles over a longer length, e.g., four times of the probe length, the twist angle then meets the acceptance criterion specified for a length no greater than 500 mm [8].

Fig. 3 shows that the systematic geometric field errors of the pre-series magnets are generally within the allowed bounds. Three pre-series magnets do have relatively large sextupoles. We installed magnetic shims in MQXFA05 to correct a_3 and b_3 and in MQXFA06 to correct a_3. It is effective to determine the application of shims based on the magnetic measurements during the magnet assembly stage, thanks to the reasonably good warm-cold correlation of the field errors as observed in previous MQXF magnets [15], [18]–[21].

The amplitude of b_6, an allowed multipole, decreased from 3.3 units in MQXFA03 to the range of 0.5–1.5 units for the following pre-series magnets (Fig. 3). This change is due to the introduction of the second-generation coils with the b_6 tuning since MQXFA04 (Table I). The b_6-tuning feature further modified the second-generation coil design [9] by changing the insulation thickness at the pole and midplane inside a coil as described in [22]. A similar reduction of b_6 is also observed in the MQXFB magnets that are being developed at CERN [22].

The rms displacement of the coil blocks, as suggested by the random part of the geometric field errors (Fig. 4), is larger than the 30–40 μm rms displacement as observed in earlier MQXFS magnets [19]. Compared to the 1.2-m long magnetic length of the MQXFS model magnets, the longer pre-series MQXFA magnets may allow an intrinsically larger coil waviness due to the tolerance of magnet fabrication tooling. If this holds, one expects a larger coil waviness also in the 7.2-m long MQXFB magnets than in the short MQXFS magnets.

Since the magnetic field generated at 10 A does not saturate

the iron load pads in the coil-pack sub-assembly, the iron yoke does not affect the field quality from the coil-pack sub-assembly to the magnet after loading. Therefore, we attribute the observed field quality change after loading (Table III and Fig. 5) to the change of the conductor positioning due to the mechanical deformation of the coils during loading. On average, an increase of 50 units of the central TF and 1.5 units of b_6 were observed in the pre-series magnets after loading. For the MQXFA magnets, one micron decrease of the inner radii of the coil blocks next to the magnet mid-planes leads to about 0.14 units of increase in the TF [23]. Therefore, the observed increase in TF can be explained by about 360 μm reduction in the inner radii of the mid-plane coil blocks during loading.

The loading also affected the low-order multipoles, namely the sextupoles and octupoles in the pre-series magnets (Table III). We note that the change in the low-order multipoles was largely due to the shift of the multipole profiles after loading (Fig. 5). This observation indicated that the loading had a stronger effect on the entire length of the coils and the positioning asymmetry among the four coils. The loading affected less the local conductor positioning that was already determined in the coil-pack sub-assembly [19].

Besides the multipoles, the loading process also affected the main-field twist angle. The data from the pre-series magnets suggested that the loading reduced the twist from the coil-pack sub-assembly, as shown in Fig. 6.

V. CONCLUSIONS

We performed the magnetic measurements on the pre-series MQXFA magnets developed by the U.S. HL-LHC AUP in collaboration with CERN. The measurements on the coil-pack sub-assemblies and magnets after loading showed that the pre-series magnets meet the acceptance criteria on the local magnetic center and main-field twist angle. The measurements necessitated the installation of magnetic shims in two pre-series magnets to correct the sextupoles and to ensure the proper field quality at the nominal operation condition. The pre-series magnets showed an rms coil block displacement of 60–70 μm, larger than the displacement of 30–40 μm as observed in the short MQXFS model magnets. The magnet loading increased the central TF and b_6 and affected the non-allowed sextupoles and octupoles in the pre-series magnets. The loading did not significantly change the local conductor positioning that was determined in the coil-pack sub-assembly. The loading reduced the main-field twist angle from the coil-pack sub-assembly to the magnet.

Although it is clear that the geometric field errors observed in the pre-series magnets are related to the asymmetry of the conductor positioning in the magnet, computationally reproducing the measured field errors remains challenging [19], [21], [24]. As the fabrication of MQXFA and other sister Nb_3Sn accelerator magnets continues, we expect to gain more data and understanding of the field quality for the accelerator magnets based on the wind-and-react Nb_3Sn technology.

ACKNOWLEDGMENT

REFERENCES

[1] G. Ambrosio, K. Amm, M. Anerella *et al.*, "Lessons learned from the prototypes of the MQXFA low-beta quadrupoles for HL-LHC and status of production in the US," *IEEE Trans. Appl. Supercond.*, vol. 31, no. 5, p. 4001105, Aug. 2021.

[2] E. Todesco, H. Bajas, M. Bajko *et al.*, "The high luminosity LHC interaction region magnets towards series production," *Superconductor Science and Technology*, vol. 34, no. 5, p. 053001, Mar. 2021.

[3] P. Ferrain, G. Ambrosio, M. Anerella *et al.*, "The HL-LHC Low-β quadrupole magnet MQXF: From short models to long prototypes," *IEEE Trans. Appl. Supercond.*, vol. 29, no. 5, p. 4001309, Aug. 2019.

[4] I. Pong, L. D. Cooley, A. Lin *et al.*, "Diameter quality control of Nb_3Sn wires for MQXF cables in the USA," *IEEE Trans. Appl. Supercond.*, vol. 29, no. 5, p. 6001505, Aug. 2019.

[5] E. F. Holik, G. Ambrosio, M. Anerella *et al.*, "Fabrication of first 4-m coils for the LARP MQXFA quadrupole and assembly in mirror structure," *IEEE Trans. Appl. Supercond.*, vol. 27, no. 4, p. 4003605, Jun. 2017.

[6] P. Ferracin, G. Ambrosio, D. Cheng *et al.*, "Assembly and pre-loading specifications for the series production of the Nb_3Sn MQXFA quadrupole magnets for the HL-LHC," this conference, THU-PO3-112-06.

[7] X. Wang, G. F. Ambrosio, D. W. Cheng *et al.*, "Field quality measurement of a 4.2-m-long prototype Low-β Nb_3Sn quadrupole magnet during the assembly stage for the High-Luminosity LHC accelerator upgrade project," *IEEE Trans. Appl. Supercond.*, vol. 29, no. 5, p. 4000706, Aug. 2019.

[8] R. Carcagno, G. Sabbi, and P. Ferracin, "Acceptance criteria part A: MQXFA magnet," October 2018, US-HiLumi-doc-1103, EDMS: 2031083, LHC-MQXFA-ES-0004.

[9] S. Izquierdo Bermudez, G. Ambrosio, A. Ballarino *et al.*, "Second-generation coil design of the Nb_3Sn low-β quadrupole for the high luminosity LHC," *IEEE Trans. Appl. Supercond.*, vol. 26, no. 4, p. 4001105, Jun. 2016.

[10] D. Cheng, G. Ambrosio, A. Ben Yahia *et al.*, "An examination of the mechanical performance of the 4.5 m long MQXFA pre-series magnets for the Hi-Lumi LHC upgrade," this conference, THU-PO3-112-01.

[11] A. K. Jain, "Basic theory of magnets," in *CERN Accelerator School: measurement and alignment of accelerator and detector magnets*, 1998, no. CERN-98-05, pp. 1–26.

[12] L. Bottura, "Standard analysis procedures for field quality measurement of the LHC magnets — part I: harmonics," LHC/MTA, Tech. Rep. LHC-MTA-IN-97-007, 2001.

[13] J. DiMarco, G. Chlachidze, A. Makulski *et al.*, "Application of PCB and FDM technologies to magnetic measurement probe system development," *IEEE Trans. Appl. Supercond.*, vol. 23, no. 3, p. 9000505, 2013.

[14] J. DiMarco, P. Akella, G. Ambrosio *et al.*, "Magnetic measurements of HL-LHC AUP cryo-assemblies at Fermilab," this conference, TUE-PO1-714-05.

[15] J. DiMarco, G. Ambrosio, G. Chlachidze *et al.*, "Magnetic measurements of the first Nb_3Sn model quadrupole (MQXFS) for the High-Luminosity LHC," *IEEE Trans. Appl. Supercond.*, vol. 27, no. 4, p. 9000105, Jun. 2017.

[16] P. Ferracin, W. Scandale, E. Todesco *et al.*, "Modeling of random geometric errors in superconducting magnets with applications to the CERN large hadron collider," *Phys. Rev. ST Accel. Beams*, vol. 3, p. 122403, 2000.

[17] S. Russenschuck, "ROXIE – a computer code for the integrated design of accelerator magnets," in *Proceedings of EPAC*, Stockholm, June 1998, pp. 2017–2019, http://www.JACoW.org.

[18] L. Fiscarelli, H. Bajas, O. Dunkel *et al.*, "Magnetic measurements on the first CERN-built models of the insertion quadrupole MQXF for HL-LHC," *IEEE Trans. Appl. Supercond.*, vol. 28, no. 3, p. 4002605, Apr. 2018.

[19] S. Izquierdo Bermudez, G. Ambrosio, H. Bajas *et al.*, "Geometric field errors of short models for MQXF, the Nb_3Sn low-β quadrupole for the high luminosity LHC," *IEEE Trans. Appl. Supercond.*, vol. 28, no. 3, p. 4006306, Apr. 2018.

[20] H. Song, J. DiMarco, A. Jain *et al.*, "Vertical magnetic measurements of the first Full-Length prototype MQXFAP2 quadrupole for the LHC Hi-Lumi accelerator upgrade project," *IEEE Trans. Appl. Supercond.*, vol. 29, no. 5, p. 4004707, Aug. 2019.

[21] H. Song, G. Ambrosio, K. Amm *et al.*, "Magnetic field measurements of first pre-series full-length 4.2 m quadrupole MQXFA03 using PCB rotating coils for the Hi-Lumi LHC project," *IEEE Trans. Appl. Supercond.*, vol. 31, no. 5, p. 4000207, Aug. 2019.

[22] S. Izquierdo Bermudez, G. Ambrosio, G. Apollinari *et al.*, "Progress in the development of the Nb_3Sn MQXFB quadrupole for the HiLumi upgrade of the LHC," *IEEE Trans. Appl. Supercond.*, vol. 31, no. 5, p. 4002007, Aug. 2021.

[23] S. Redaelli, "Analysis of the magnetic field perturbations in dipoles and quadrupoles of the Large Hadron Collider (LHC)," Ph.D. dissertation, The University of Milan, 2000.

[24] E. F. Holik, G. Ambrosio, A. Carbonara *et al.*, "Field quality and fabrication analysis of HQ02 reconstructed Nb_3Sn coil cross sections," *IEEE Trans. Appl. Supercond.*, vol. 27, no. 4, p. 4003405, Jun. 2017.